



Martian environmental chamber: Dust system injection

F. Cozzolino^{a,*}, V. Mennella^a, A.C. Ruggeri^a, G. Mongelluzzo^{a,b}, G. Franzese^a, C.I. Popa^a,
C. Molfese^a, F. Esposito^a, C. Porto^a, D. Scaccabarozzi^c

^a INAF – Osservatorio Astronomico di Capodimonte, Salita Moiaro 16, 80131, Napoli, Italy

^b Department of Industrial Engineering, University of Naples “Federico II”, Piazzale Tecchio 80, 80125, Napoli, Italy

^c Department of Mechanical Engineering Politecnico of Milano, via Gaetano Previati, 1/c, 23900, Lecco, Italy

ARTICLE INFO

Keywords:

Dust
Mars
Injection
Airborn dust
MicroMED ExoMars
Martian atmosphere
Particle counter

ABSTRACT

The aim of this work is to describe the development and implementation of an experimental setup able to reproduce some characteristics of the Martian atmosphere. The development of such setup fits into the context of MicroMED project, that foresees the development of an optical particle counter to be accommodated on the ExoMars 2020 Surface Platform, as part of the suite of sensors named Dust Complex. MicroMED will perform the first direct measurement of the size distribution of the powder close to Martian surface. The experimental setup is able to reproduce the characteristics of the Martian atmosphere: pressure, atmospheric composition, the actual temperature in which MicroMED will operate (from $-20\text{ }^{\circ}\text{C}$ to $40\text{ }^{\circ}\text{C}$) and the most important thing: *the presence of suspended dust*.

The main result obtained in this work was the right configuration of an experimental setup in which to test sensors or instruments that work in Martian conditions. In particular, a dust injection system has been developed in order to obtain a dust distribution that was localized and without the formation of particles aggregates, for a correct calibration of the instrument.

1. Introduction

For years, dust on Mars has stirred the interest of the scientific community being the protagonist of many phenomena observed on the planet. For example, dust absorbs and scatters solar radiation, strongly modifying atmospheric thermal structure and balance. The most spectacular events related to the presence of dust that can be observed on Mars are local and global sandstorms and dust devils. The mechanisms of transport and distribution of these phenomena are not yet well determined by models (Kahre, 2006; Newman, 2002; Taylor, 2007) because, unfortunately, there is a lack of information on the physical characteristics of the grains such as size distribution and concentration.

The only information available to investigate the physical characteristics of powder has been provided by light absorbance measurements. Indeed, measuring the optical depth with complex calculations and making strong assumptions on the shape, on the grains refractive index, it is possible to obtain the effective radius of the airborne dust distribution.

Currently, there are different observations of the dust haze, performed by using both the surface and orbital images (Toon et al., 1977; Drossart et al., 1991; Pollack et al., 1995; Tomasko et al., 1999; Greeley

et al., 2006; Vasilyev et al., 2009; Fedorova et al., 2009; Vicente-Retortillo et al., 2017), but any direct measurement of the airborne dust has been performed yet.

To provide a direct measurement of airborne dust, the optical particle counter MicroMED has been developed to be capable of operating in Martian atmospheric conditions (see f.e. Scaccabarozzi et al., 2018). MicroMED has been selected for the ExoMars 2022 Mission, onboard the Surface Platform. The instrument is based on the light diffusion principle and is able to aspire the suspended dust, measuring its size distribution and abundance by analyzing the single grain scattered light. It will operate directly close to the surface, where dust is lifted, allowing monitoring of the dust injection into the atmosphere. MicroMED is part of the Dust Complex, a suite of five sensors devoted to the study of Martian dust. In addition to MicroMED, the suite hosts a Conductivity Sensor, Impact Sensor, Electric Probes and an Electro Magnetic-sensor. This set of instruments will allow to study the processes linked to the lifted dust as f.e., the induced electrical field. Indeed, airborne dust tends to acquire charge from triboelectrification, a process that depends on the grains composition and size (Kunkel, 1950; McCarty and Whitesides, 2008; Melnik and Parrot, 1998; Desch and Cuzzi, 2000), as well on the

* Corresponding author.

E-mail address: fabio.cozzolino@inaf.it (F. Cozzolino).

environmental conditions (Esposito et al., 2016, Harrison, 2016; Neakrase, 2016; Murphy, 2016). Dust charging can lead to strong electric field, in theory able to overcome the Martian electric breakdown (Farrell et al., 2017; Franzese et al., 2018).

In order to verify the performances and calibrate MicroMED, it was necessary to recreate the atmospheric conditions that the instrument will find on Mars, in particular the presence of dust. The response of MicroMED to this condition has been simulated using a CFD (Computational Fluid Dynamics) analysis in order to understand what are the critical parameters and the range of variation to be guaranteed in laboratory (Mongelluzzo et al., 2018). In order to reproduce the Martian conditions, a simulator chamber has been developed in which it is possible to recreate the Mars atmospheric composition, pressure, temperature and dust concentration that MicroMED will face during its operative time. Obviously, this type of setup can be used for the calibration of different instruments such as impact sensors, microbalances and optical particle counters.

2. Mars atmosphere simulator

To recreate the atmospheric conditions of Mars in order to verify the performances of MicroMED, a cylindrical vacuum chamber has been used, called simulation chamber, as shown in Fig. 1.

The average pressure on Mars is around 7–8 mbar (Zurek et al., 1992; Martinez G.M et al., 2017). This value was obtained in the simulation chamber, using a pumping system consisting of two cascade pumps: a Varian Tri_Scroll 600 Series Dry Scroll and a Turbo V-750 Twis Torr. The pumping system can generate a maximum vacuum of about 10⁻⁴ mbar in the chamber, therefore suitable for reproducing the Martian pressure regime. The Scroll pump is also equipped with a VPI valve that blocks the flow in the direction of the pump when it stops functioning. Pressure monitoring is performed through the Pfeiffer compact capacitance gauge with a measurement range of 0–1000 mbar. The sensor is connected to an external controller that displays the value of the pressure in the chamber. In prevision of a MicroMED testing campaign, the chamber had to allow the injection of dust grains of different sizes. In particular, in order to test the response of the instrument to calibrated monodispersed grains, these have to remain separated from others. Indeed, the electrification of the grains could lead to the formation of aggregates, that in turn alter the size distribution in input introducing a further level of uncertainty.

An injection system has been realized capable of injecting a flow of thousands of separated grains inside the chamber. The injection system

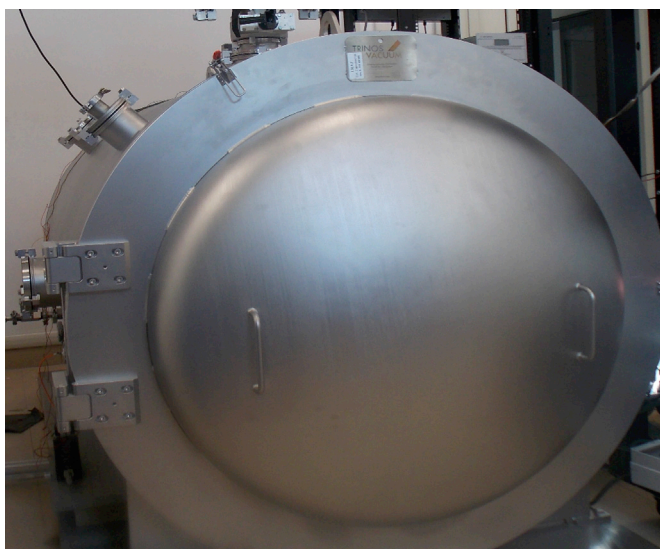


Fig. 1. Vacuum chamber to simulate the Martian atmosphere.

had been developed and improved through several intermediate steps, before obtaining the desired performance.

3. Dry injection system

The first injection system, named Dry Injection, was made up of a holder containing the dry particles, connected to the chamber through a gate valve. When the valve is opened, due to the pressure difference between the holder (ambient pressure) and the chamber (1 mbar), the particles are aspirated into the chamber.

This injection system shows two problems:

- 1) *The flux of particles is focused in a very restricted area inside the chamber, so it is not uniformly distributed.*
- 2) *The formation of groups of aggregated particles that represents a critical issue for the calibration of the MicroMED optical particle counter.*

In order to verify the reliability of the system, several tests have been performed. To monitor the distribution of grains inside the chamber, various aluminum stubs have been deployed on its base as shown in Fig. 2. Each stub was covered with an adhesive carbon disc on which the injected particles could sediment. All carbon discs were then analyzed with a Scanning Electronic Microscope (SEM).

Some samples, observed using SEM, are shown in Fig. 3 (single aggregate) and Fig. 4 (multiple aggregates). The formation of particle aggregates using the Dry Injection System is evident.

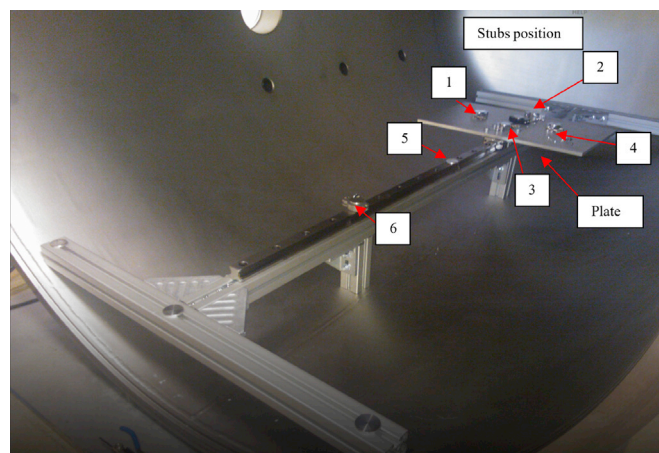


Fig. 2. Aluminum Stub with Carbon Disc inside the simulation chamber.

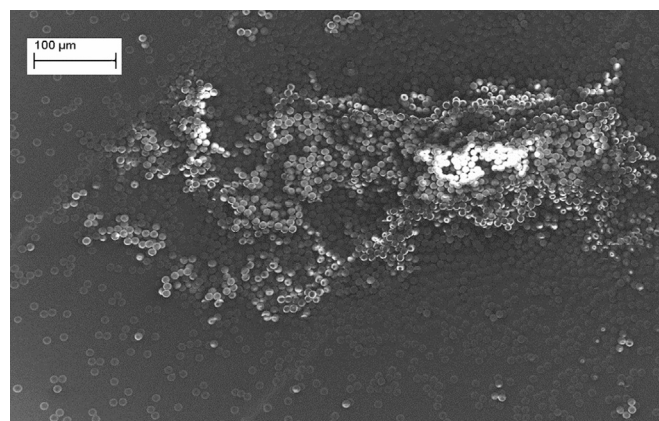


Fig. 3. Local concentration of particles injected with dry system as observed over carbon stubs at the SEM.

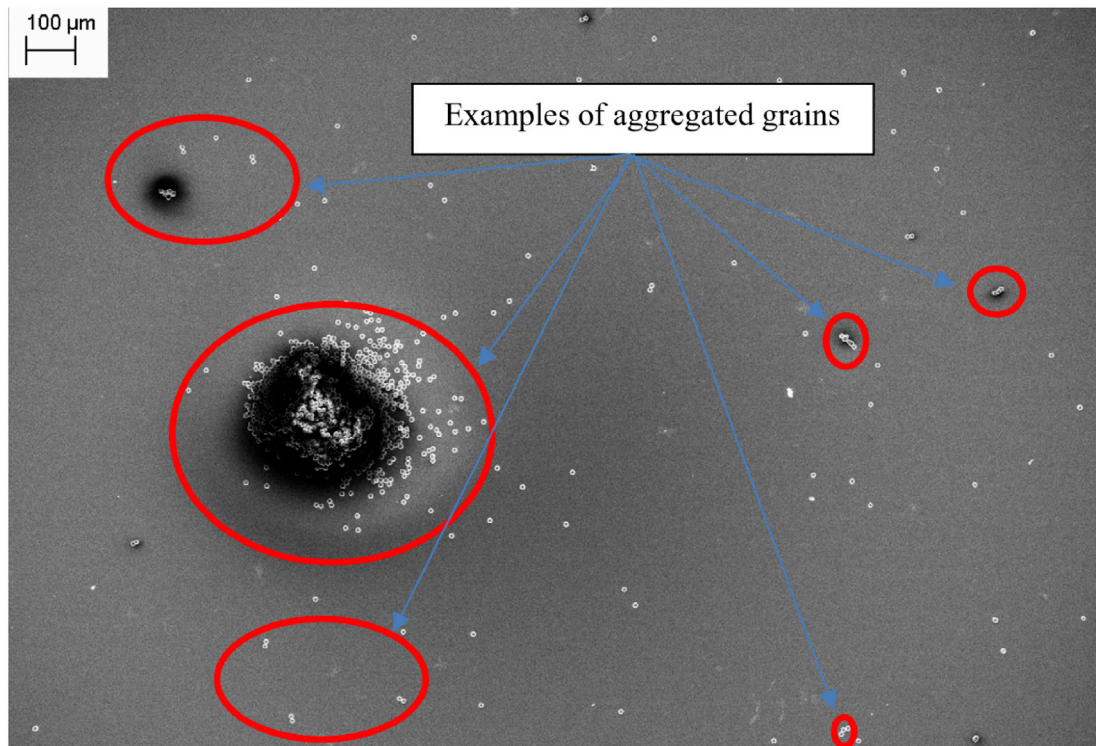


Fig. 4. Evidence of particles aggregation in the chamber after injection of dry particles.

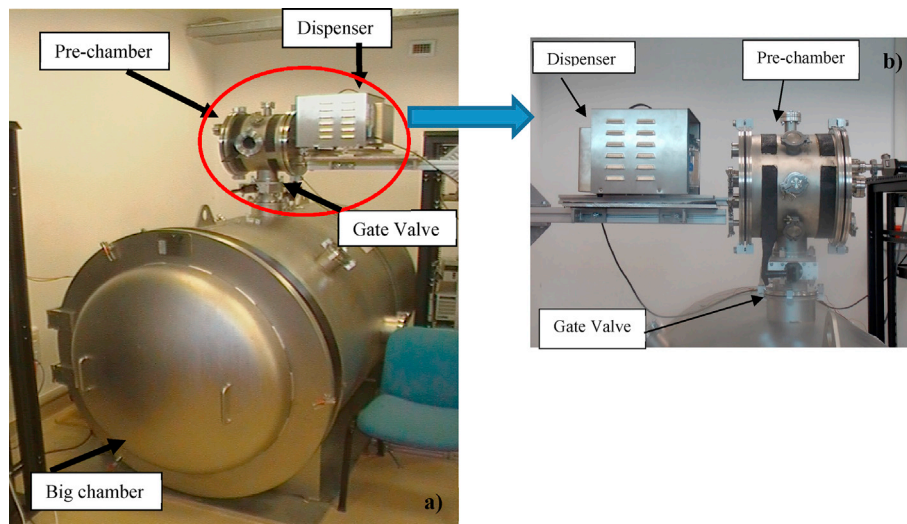


Fig. 5. Martian Simulation chamber. a) The complete system; b) "Wet" injection system.

4. Wet Injection System

In order to solve the problem of the particle aggregates presented in the Dry Injection System, a different injection system has been developed, using grains embedded in a solution.

The system shown in Fig. 5 is constituted by a dispenser (Grimm Aerosol Dispensers mod 7811), a second vacuum cylindrical chamber (pre-chamber), considerably smaller than the Martian vacuum chamber, and a gate valve.

The used aerosol generator is shown in Fig. 6. It nebulizes a solution consisting of water and particles to be injected into the pre-chamber. The nebulization is the reduction of a liquid in very small parts (drops), which is obtained, for example, by colliding the liquid with a jet of air at high speed, or forcing the liquid to pass through a very narrow orifice.

Before the nebulization, the solution is placed in an ultrasonic

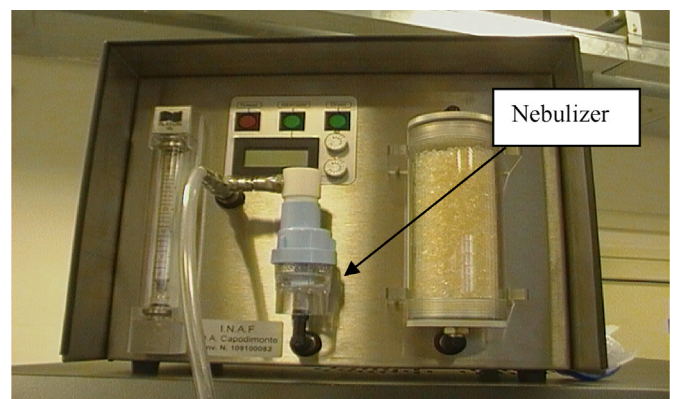


Fig. 6. Particle generator model 7.811.

Table 1

Features of Grimm mod 7.811 Particle-Generator.

Supply Voltage	240 V	Aerosol Substance	Aqueous solutions
Frequency	50–60 Hz	Nebulizer flow rate	2.5 [l/min] to 7.0 [l/min]
Maximum current	1.7 A	Dryer flow rate	7.5 [l/min] to 17 [l/min]
Temperature Range	0 [°C] to 40 [°C]	Nebulizer liquid capacity	3 [ml] to 10 [ml]
Aerosol output air pressure range	Equal to atmospheric pressure	Particle concentration	$\geq 10^7$ [1/cm ³]
Maximum relative Humidity	90 [%] non condensing	Particle size range	50 [nm] to 5000 [nm]

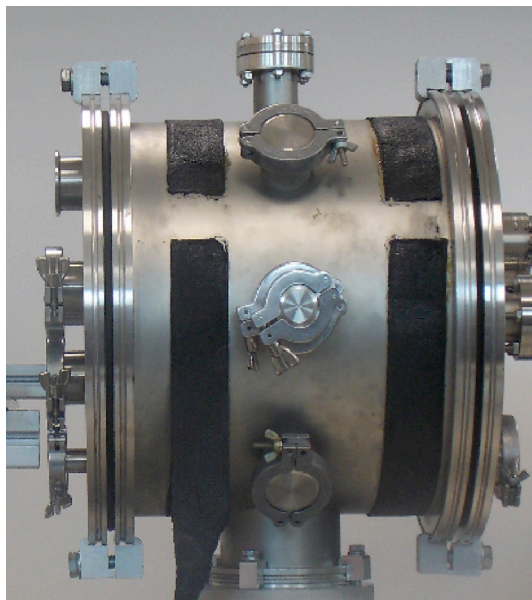


Fig. 7. Vacuum pre-chamber.

chamber in order to well separate the embedded grains.

Nebulizer flow rate is adjustable. The maximum flow rate is 7 l/min and is reachable at 1 atm pressure. For our tests, we set the flow rate at 7 l/min. The features of dispenser are summarized in Table 1.

The pre-chamber has dimensions of 30 cm in diameter \times 25 cm in height. The injection system is connected to the top of the first chamber. Between the second and the first chamber one there is the gate valve as shown in Fig. 5. The gate valve is operated by hand.

4.1. Vacuum pre-chamber

The vacuum pre-chamber (Fig. 7) is a steel cylinder and with four flanges on upper base: three DN40 and one DN15. On its side there are four flanges DN40 and two DN100. On the lower base there are three

DN40 and one DN15. All flanges are Iso K. The flanges we used are: one DN15 on the upper base connected to the output of the aerosol generator, one DN100 where the valve connected to a manual gate and a DN100-DN15 flange reducing connected with the pipe coming from the large chamber (Martian Simulation Chamber). The rest of the flanges have been closed with blind flanges.

The pressure in the pre-chamber will be 1 atm as required by the characteristics of the particle generator.

4.2. Big vacuum chamber (Martian Simulation Chamber)

The big vacuum chamber, where MicroMED will be tested, is a steel cylinder with 1.34 m in diameter and 2.05 m in length. It is provided on the upper part of a window DN160 and three flanges DN15 to one of which will be connected to the pipe coming from the pre-chamber. On the side there are 2 windows DN160, 3 flanges DN60, one of which will be used to feedthrough liquids for a future cooling system, 2 flanges DN100 to one of which will be connected with a flange feedthrough that will allow us to power with 6 V the MicroMED pump from the outside. The internal pressure will be increased to 6 mbar using a scroll pump Agilent mod TS600 220V 1 Ph. The chamber is provided of an internal moving aluminum panel that can slide on a track system in order to set its position. During the phase of testing, MicroMED will be placed on this base. The vacuum chamber is connected to the vacuum pre-chamber by a steel tube, which will guide the passage of the particles in the main chamber.

5. Measurements of particle distribution in Martian simulation chamber

Once the Simulator Chamber was implemented, a series of measurements were carried out to verify the functionality of the injection system and the distribution of the particles in the simulation chamber. Aluminum stubs have been positioned same as above mentioned (Fig. 2). The injection system generates an aerosol of particles that is distributed inside the pre-chamber.

When the gate is opened, due to the difference in pressure between the simulation chamber (1 mbar) and pre-chamber (1 atm) the particles are sucked with high speed into the simulation chamber. The particles

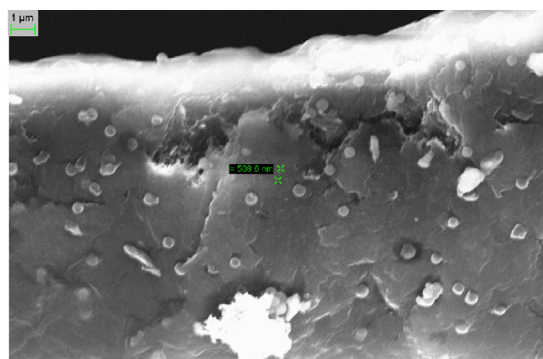
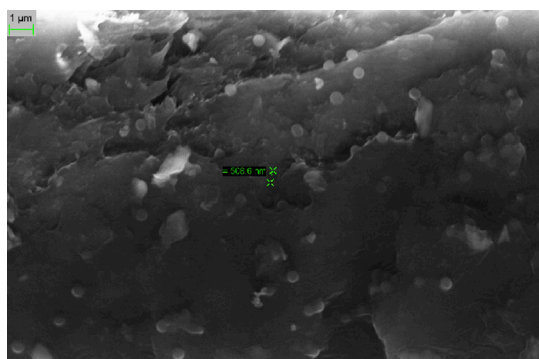


Fig. 8. Absence of aggregates particles injected with the Wet Injection System.

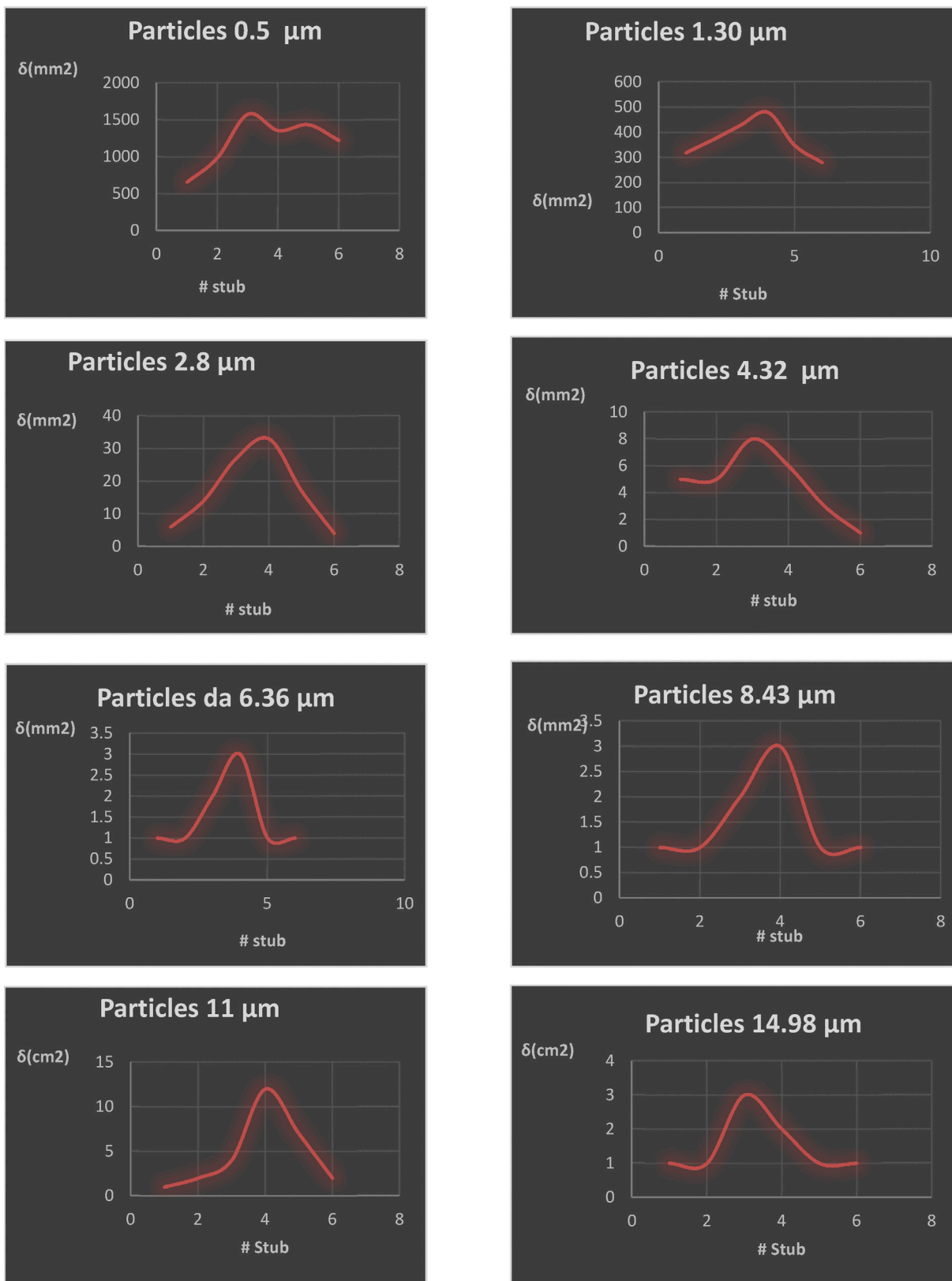


Fig. 9. Particle distribution according to the position of the sampling discs positioned in the simulation chamber. Y-axis shows the density value, while x-axis the position of the disks.

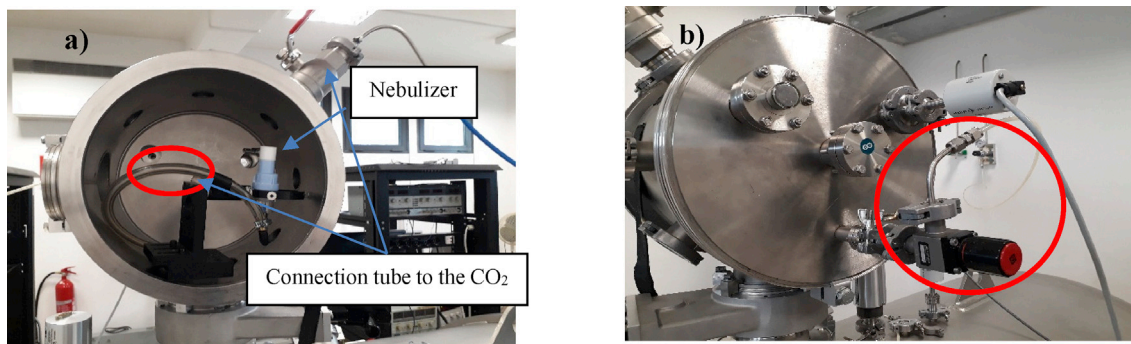


Fig. 10. a) Nebulizer inside the pre-chamber connected to system injected of CO2 b) System injected of CO2.

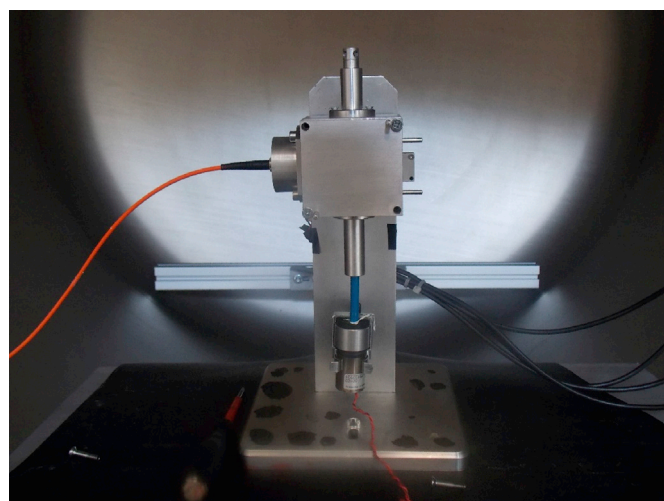


Fig. 11. BreadBoard version of MicroMED installed in the simulation chamber.

bounce on the bottom of the chamber and are spread. Once the equilibrium condition of 6 mbar is reached, the bounced particles deposit for gravity on the discs positioned at the base of the chamber. At the end of the settling process the disks are analyzed with the SEM. The disks have been numbered, each corresponding to a precise position within the chamber. In particular, the disks 3, 4, and 5 have been positioned at the gate valve which represents the entry of the particles in the simulation chamber. The disks 1, 2 and 6 have been positioned respectively at 1 m from the disk 3, at 0.7 m from disk 3 and 0.15 cm from disk 5.

The test was performed using monodispersed particles with size 0.5, 1.30, 2.8, 4.32, 6.36, 8.43, 11, 14.98 μm .

The same set of particles has been used during the calibration of MicroMED. From the analysis of the stubs to the SEM it is evident that injecting the particles with this injection system avoids the formation of the aggregates of particles that were present with the dry injection system, as shown in Fig. 8.

The results about distribution particles inside the big chamber are shown in Fig. 9, where is shown the trend of the numerical density of the particles as a function of the position of the disks, for each used particle size.

Table 2

The results in volt of the MicroMED BreadBoard acquisitions for the test with monodispersed spherical grains.

Channel	Size (μm)	Number	Mean (V)	Median (V)	Standard Deviation (V)	Lower Quartile (V)	Upper Quartile (V)
High	0.448	150	0.18	0.17	0.09	0.11	0.25
High	1.046	113	2.4	1.9	1.7	1.2	3.4
Low	4.051	135	0.18	0.15	0.19	0.09	0.20
Low	8.496	145	0.47	0.29	0.49	0.18	0.52

The plots show that the “wet” injection is able to spread well the dust grains into the simulation chamber on the whole size range considered. The smaller particles tend to disperse more, distributing almost uniformly throughout the chamber, while the larger diameter particles tend to be distributed in the region corresponding to their entrance area (the area under the gate valve).

The injection system that makes use of the dispenser has a limitation, because it only works in presence of 1 bar atm, so it can inject particles into the pre-chamber only if it has a pressure of 1 bar. The consequence of this is that when the gate valve between the pre-chamber and the simulation chamber is opened, the strong pressure difference causes the particles to acquire a very high speed, so to bounce on the chamber bases and wall before being sampled by MicroMED. This causes a large dispersion and loss of particles. To improve this aspect, the particle injection system has been simplified in order to control the input velocity of the particles in the simulation chamber. As shown in Fig. 10, the Grimm dispenser was removed and just the nebulizer was placed, filled up with a solution of ethanol and particles, inside the pre-chamber connecting it to the CO2 injection system of the chamber. This configuration allows to inject the particles after having depressurized the pre-chamber (for example, bringing it to 15–16 mbar) with a pump, in order to control the pressure gap between the two chambers, as well as the particle velocity.

We used ethanol instead of water for the particles solution in order avoid the freezing during the rapid gas expansion experienced caused by the gate opening. Ethanol is a very volatile liquid which evaporates at a pressure of 6 mbar and with a temperature of about 22 °C, depositing on the walls of the chamber. Various measurements were made by injecting only ethanol to understand if the droplets that are generated could somehow be sucked. Test results show that MicroMED does not reveal ethanol.

6. MicroMED BreadBoard performance test

Using the results presented in the last section, it was possible to identify the optimal position where the grains concentration peaks. In this position, corresponding to the disks 3 and 4, we installed a BreadBoard version of MicroMED, as shown in Fig. 11, in order to perform the first tests of the sensor performances.

The tests performed with the upgraded injection system showed an increase in the number of particles acquired by MicroMED.

Table 2 shows the average amplitudes of the signals generated by the particles sucked by MicroMED, for grain size of 0.448, 1.046, 4.051,

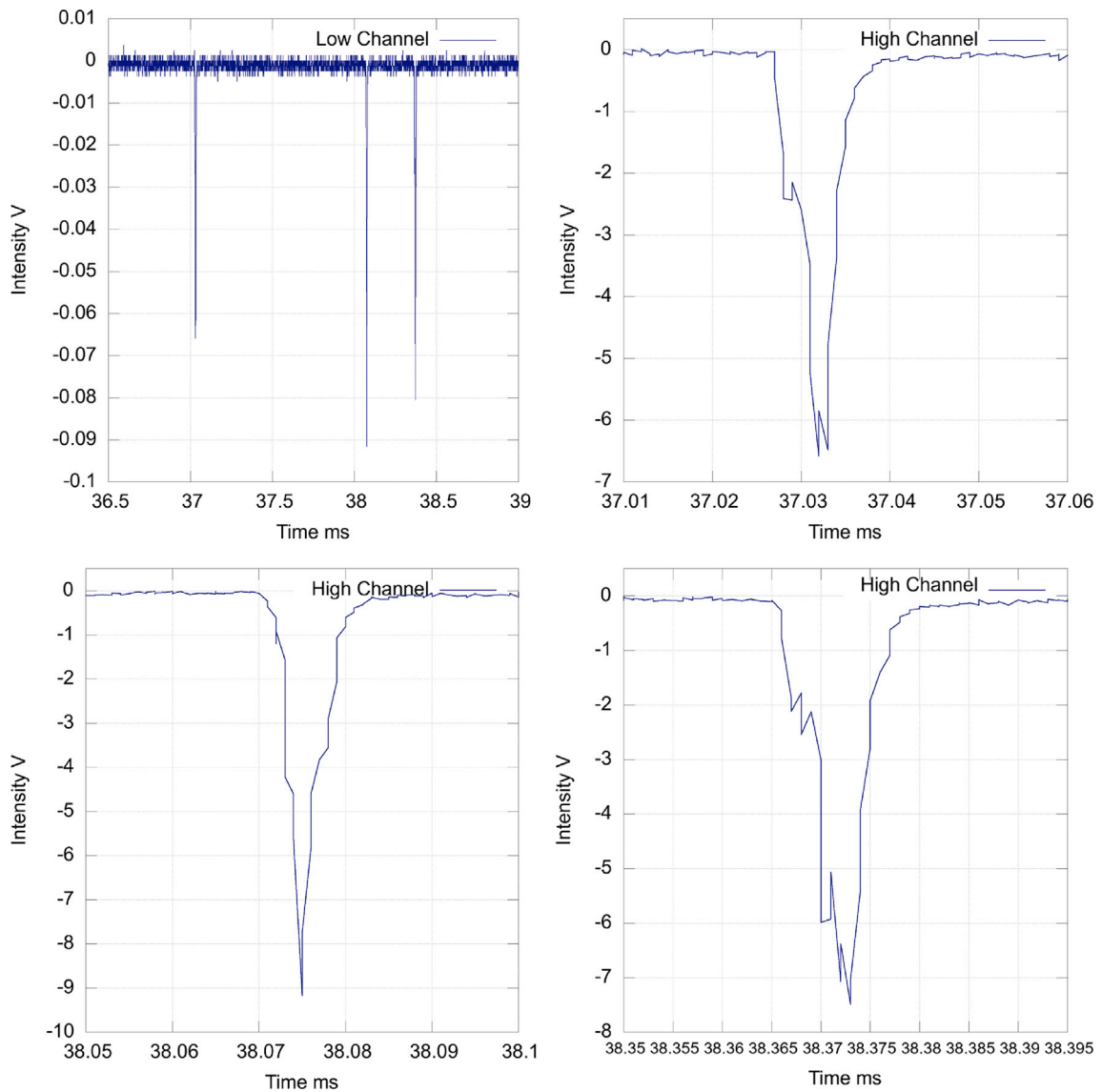


Fig. 12. Example of the signals acquired by MicroMED BreadBoard. The first plot on top left shows an extract of the time series acquired in Low channel during the particles injection: three passing grains are visible. The successive plots show a zoom of these three signals in High channel.

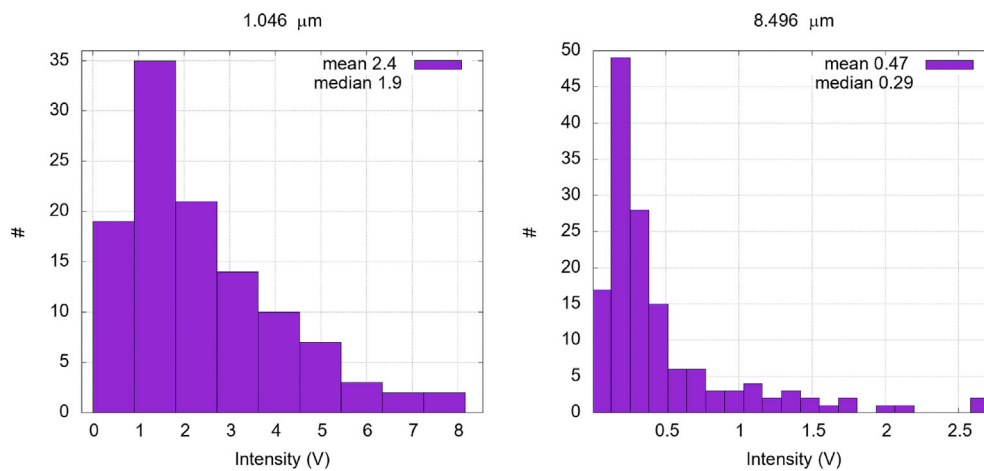


Fig. 13. Intensity distribution of the signals acquired in by MicroMED BreadBoard: left) High Channel for the injection of a monodispersed samples of 1.046 μm spherical grains; right) Low Channel for the injection of a monodispersed samples of 8.496 μm spherical grains.

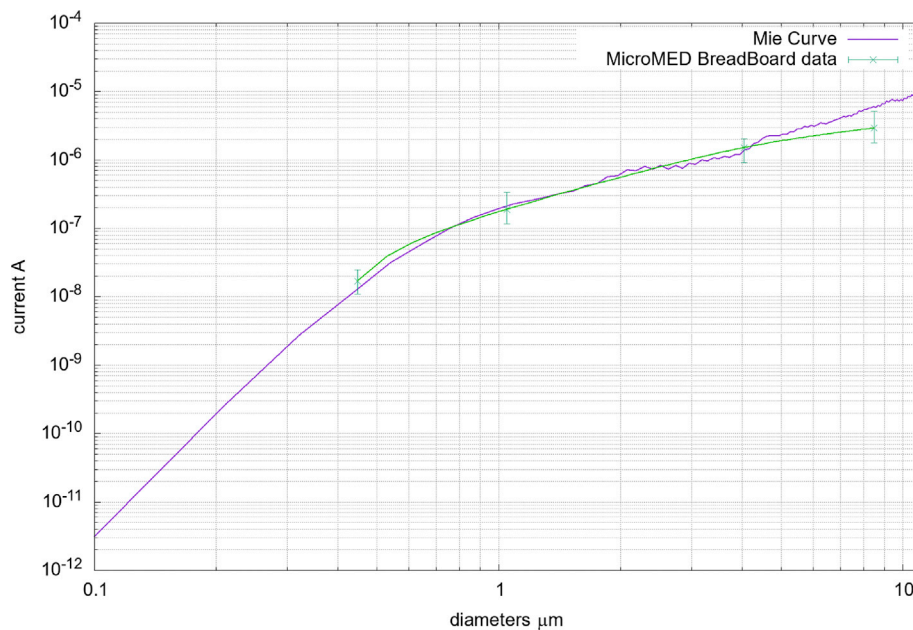


Fig. 14. Comparison of the signals current obtained from the MicroMED BreadBoard measurements and the average theoretical Mie curve expected.

8.496 μm . The particle signals were acquired using an electronic board having two channels with different amplification stage called Low and High. The Low channel was used for the study of the signals of the particles with a diameter greater than 2 μm and had an amplification factor of 105, while the High channel was used for the study of the signals of the particles with a diameter less than 2 μm and had the amplification factor of 107.

An example of the signals acquired by MicroMED BreadBoard in both channels is shown in Fig. 12.

In Fig. 13, two amplitude distribution of signals for High and Low channels are shown.

The average values of the amplitudes, reported in Table 2, were compared with the theoretical instrumental response of MicroMED, obtained from the Mie model. A good agreement between the theoretical and experimental trend can be seen in Fig. 14.

7. Conclusions

The next ESA/Roscosmos ExoMARS 2020 missions aim to investigate possible life traces on the Martian surface and study the Martian past and present climate, in order to address its sustainability for the life. To achieve this goal, it is fundamental to perform a proper characterization of the atmospheric dust and its interactions with the Martian weather.

MicroMED is an optical particle counter on board of the surface lander, as part of the Dust Complex, a suite of instruments aimed to the study of the characteristics of the primary lifted dust. In particular, MicroMED will acquire the first direct measurement of the primary dust amount and size distribution.

In order to develop the instrument, we realized a Martian simulation chamber able to reproduce the environment where MicroMED will operate. Here, the most important goal reached has been the development of the correct configuration of the injection dust system, in order to obtain a dust distribution without aggregations and localized near the instrument.

The Dust Injection System is constituted by a system of vacuum chambers that allows the injection of dust particles in a controlled CO₂ low pressure environment. We decided to inject the dust grains inside the chamber in an ethanol solution, in order to generate a flux of particles without aggregations.

Indeed, the ethanol acts as a protective membrane for particles preventing triboelectric effects that cause aggregations.

With this new injection system, the following improvements are reached:

- 1) the possibility to vary the flow velocity by acting on the pressure gradient between the pre-chamber and the simulation chamber;
- 2) the direct injection of CO₂ and particles to simulate the Martian atmosphere;
- 3) the avoidance of particles loss.

The Martian simulation chamber is currently used during the development of the MicroMED for tests and calibrations.

Declaration of competing interest

The authors declare that they have no known competing financial interests or personal relationships that could have appeared to influence the work reported in this paper.

CRediT authorship contribution statement

V. Mennella: Supervision. **G. Franzese:** Formal analysis. **F. Esposito:** Supervision.

Acknowledgment

This work has been supported by ASI (contract's grant number: 2016/41/H.0). The instrument development was funded and coordinated by ASI under the scientific leadership of INAF-Naples, Italy. The data used in this paper can be accessed upon personal request to the first author (fabio.cozzolino@inaf.it).

Appendix A. Supplementary data

Supplementary data to this article can be found online at <https://doi.org/10.1016/j.pss.2020.104971>.

References

- Desch, S.J., Cuzzi, J.N., 2000. The generation of lightning in the solar nebula. *Icarus* 143 (1), 87–105.
- Drossart, P., et al., 1991. Martian aerosol properties from the Phobos/ISM experiment. *Ann. Geophys.* 9, 754–760.

- Esposito, F., Molinaro, R., Popa, C.I., Molfese, C., Cozzolino, F., Marty, L., et al., 2016. The role of the atmospheric electric field in the dust-lifting process. *Geophys. Res. Lett.* 43 (10), 5501–5508.
- Farrell, W.M., McLain, J.L., Collier, M.R., Keller, J.W., 2017. The Martian dust devil electron avalanche: laboratory measurements of the E-field fortifying effects of dust-electron absorption. *Icarus* 297, 90–96.
- Fedorova, A.A., et al., 2009. Solar infrared occultation observations by SPICAM experiment on Mars-Express: simultaneous measurements of the vertical distributions of H₂O, CO₂ and aerosol. *Icarus* 200, 96–117. <https://doi.org/10.1016/j.icarus.2008.11.006>.
- Franzese, G., Esposito, F., Lorenz, R., Silvestro, S., Popa, C.I., Molinaro, R., et al., 2018. Electric properties of dust devils. *Earth Planet Sci. Lett.* 493, 71–81.
- Harrison, et al., 2016. Applications of electrified Dust and dust devil Electrodynamics to martian atmospheric electricity. *Space Sci. Rev.* 203 (2016), 299–345.
- Kahre, et al., 2006. Modeling the Martian dust cycle and surface dustreservoirs with the NASA Ames general circulationmodel. *J. Geophys. Res.* 111, E06008.
- Kunkel, W.B., 1950. The static electrification of dust particles on dispersion into a cloud. *J. Appl. Phys.* 21 (8), 820–832.
- McCarty, L.S., Whitesides, G.M., 2008. Electrostatic charging due to separation of ions at interfaces: contact electrification of ionic electrets. *Angew. Chem., Int. Ed. Engl.* 47 (12), 2188–2207.
- Melnik, O., Parrot, M., 1998. Electrostatic discharge in Martian dust storms. *J. Geophys. Res. Space Phys.* 103 (A12), 29107–29117.
- Mongelluzzo, G., Esposito, F., Cozzolino, F., Molfese, C., Silvestro, S., Popa, C.I., et al., 2018, June. Optimization of the fluid dynamic design of the Dust Suite-MicroMED sensor for the ExoMars 2020 mission. In: 2018 5th IEEE International Workshop on Metrology for Aerospace (MetroAeroSpace). IEEE, pp. 134–139.
- Murphy, et al., 2016. Field Measurements of Terrestrial and martian dust devils. *Space Sci. Rev.* 203 (2016), 39–87.
- Neakrase, et al., 2016. Particle lifting Processes in dust devils. *Space Sci. Rev.* 203 (2016), 347–376.
- Newman, et al., 2002. Modeling the Martian dust cycle, 1. *Representations of dust transport processes.* *J. Geophys. Res.* 107 (E12), 5123.
- Pollack, J.B., et al., 1995. Viking Lander image analysis of Martian atmospheric dust. *J. Geophys. Res.* 100, 5235–5250. <https://doi.org/10.1029/94JE02640>.
- Scaccabarozzi, Diego, et al., 2018. MicroMED, design of a particle analyzer for Mars. *Measurement* 122, 466–472.
- Taylor, et al., 2007. Modelling dust distributions in the atmospheric boundary layer on Mars. *Boundary-Layer Meteorol.* 125 (2007), 305–328.
- Tomasko, M.G., et al., 1999. Properties of dust in the martian atmosphere from the imager on Mars pathfinder. *J. Geophys. Res.* 104, 8987–9008. <https://doi.org/10.1029/1998JE900016>.
- Toon, O.B., et al., 1977. Physical properties of the particles composing the Martian dust storm of 1971-1972. *Icarus* 30, 663–696. [https://doi.org/10.1016/0019-1035\(77\)90088-4](https://doi.org/10.1016/0019-1035(77)90088-4).
- Vasilyev, A.V., Mayorov, B.S., Bibring, J.-P., 2009. The retrieval of altitude profiles of the Martian aerosol microphysical characteristics from the limb measurements of the Mars Express OMEGA spectrometer. *Sol. Syst. Res.* 43 (5), 392–404.
- Vicente-Retortillo, Á., Martínez, G.M., Renno, N.O., Lemmon, M.T., de la Torre-Juárez, M., 2017. Determination of dust aerosol particle size at Gale Crater using REMS UVS and Mastcam measurements. *Geophys. Res. Lett.* 44 <https://doi.org/10.1002/2017GL072589>.
- Zurek, R.W., Barnes, J.R., Haberle, R.M., Pollack, J.B., Tillman, J.E., Leovy, C.B., 1992. Dynamics of the Atmosphere of Mars, pp. 835–933. Mars.